

Undulated short-tail* Deletion Mutation in the Mouse Ablates *Pax1* and Leads to Ectopic Activation of Neighboring *Nkx2-2* in Domains That Normally Express *Pax1

Chikara Kokubu,^{*,1,2} Bettina Wilm,^{*,1,3} Tomoko Kokubu,^{*} Matthias Wahl,^{*} Isabel Rodrigo,^{*} Norio Sakai,^{*} Fabio Santagati,^{*} Yoshihide Hayashizaki,[†] Misao Suzuki,[‡] Ken-ichi Yamamura,[§] Kuniya Abe^{} and Kenji Imai^{*,4}**

^{*}GSF-National Research Center for Environment and Health, Institute of Developmental Genetics, 85764 Neuherberg, Germany,

[†]RIKEN Genomic Sciences Center, RIKEN Yokohama Institute, Yokohama 230-0045, Japan, [‡]Center for Animal Resources and Development and [§]Institute of Molecular Embryology and Genetics, Kumamoto University School of Medicine, 862-0976 Kumamoto, Japan and ^{**}Technology and Development Team for Mammalian Cellular Dynamics, RIKEN Tsukuba Institute, BioResource Center, Ibaraki 305-0074, Japan

Manuscript received February 13, 2003

Accepted for publication May 27, 2003

ABSTRACT

Previous studies have indicated that the *Undulated short-tail* deletion mutation in mouse *Pax1* (*Pax1*^{U^{ns}}) not only ablates *Pax1*, but also disturbs a gene or genes nearby *Pax1*. However, which gene(s) is involved and how the *Pax1*^{U^{ns}} phenotype is confined to the *Pax1*-positive tissues remain unknown. In the present study, we determined the *Pax1*^{U^{ns}} deletion interval to be 125 kb and characterized genes around *Pax1*. We show that the *Pax1*^{U^{ns}} mutation affects four physically linked genes within or near the deletion, including *Pax1*, *Nkx2-2*, and their potential antisense genes. Remarkably, *Nkx2-2* is ectopically activated in the sclerotome and limb buds of *Pax1*^{U^{ns}} embryos, both of which normally express *Pax1*. This result suggests that the *Pax1*^{U^{ns}} deletion leads to an illegitimate interaction between remotely located *Pax1* enhancers and the *Nkx2-2* promoter by disrupting an insulation mechanism between *Pax1* and *Nkx2-2*. Furthermore, we show that expression of *Bapx1*, a downstream target of *Pax1*, is more strongly affected in *Pax1*^{U^{ns}} mutants than in *Pax1*-null mutants, suggesting that the ectopic expression of *Nkx2-2* interferes with the *Pax1*-*Bapx1* pathway. Taken together, we propose that a combination of a loss-of-function mutation of *Pax1* and a gain-of-function mutation of *Nkx2-2* is the molecular basis of the *Pax1*^{U^{ns}} mutation.

AN allelic series of mutations can provide important tools for understanding gene function and regulation. Earlier studies have demonstrated that three spontaneous mouse mutations constitute an allelic series in *Pax1*: *undulated* (*Pax1*^{un}; WRIGHT 1947), *undulated-extended* (*Pax1*^{un-ex}; WALLACE 1980), and *Undulated short-tail* (*Pax1*^{U^{ns}}; BLANDOVA and EGOROV 1975). *Pax1* is a member of the Pax gene family, which consists of transcription factors characterized by the presence of a highly conserved DNA-binding domain, the paired box (DAHL *et al.* 1997; MANSOURI *et al.* 1999). Embryonic expression of *Pax1* is detected in the sclerotome of somites from embryonic day (E) 8.5 (DEUTSCH *et al.* 1988; WALLIN *et*

al. 1994), the pharyngeal pouch endoderm from E9.5 (WALLIN *et al.* 1996), and limb buds from E10.0 (TIMMONS *et al.* 1994). The recessive *Pax1*^{un} allele has a point mutation in the paired box (BALLING *et al.* 1988), while the recessive *Pax1*^{un-ex} and the semidominant *Pax1*^{U^{ns}} alleles carry deletion mutations (WALLIN *et al.* 1994; DIETRICH and GRUSS 1995). In each allele, affected mice display dysmorphologies as developmental defects in the derivatives of embryonic *Pax1*-positive tissues, including the vertebral column, the shoulder girdle, the sternum (GRÜNEBERG 1950, 1954), and the thymus (DIETRICH and GRUSS 1995; WALLIN *et al.* 1996). Notably, the three alleles differ significantly in the severity of their phenotypes and in the mode of inheritance, raising a question as to how each mutation correlates with the respective phenotypes. To address this question, we have previously created a targeted null allele of *Pax1* (*Pax1*^{null}) and made a phenotypic comparison between the natural alleles and the *Pax1*^{null} allele as a reference (WILM *et al.* 1998). This analysis has demonstrated that *Pax1*^{un} is a hypomorphic allele, while *Pax1*^{un-ex} can be regarded as a null allele. In contrast, the *Pax1*^{U^{ns}} deletion mutation, which removes all exons of *Pax1* (DIETRICH and GRUSS 1995; WALLIN *et al.* 1996), displays a significantly stronger phenotype than *Pax1*^{null} displays,

Sequence data from this article have been deposited with the EMBL/GenBank Data Libraries under accession nos. AF285175, AB080656, AB080657, and AB080658.

¹These authors contributed equally to this work.

²Present address: Graduate School of Frontier Biosciences, Osaka University, Suita, Osaka 565-0871, Japan.

³Present address: Division of Cardiovascular Medicine, Vanderbilt School of Medicine, Nashville, TN 37232.

⁴Corresponding author: GSF-National Research Center for Environment and Health, Institute of Developmental Genetics, Ingolstädter Landstr. 1, D-85764 Neuherberg, Germany. E-mail: imai@gsf.de

indicating that the *Pax1*^{Uns} mutation affects not only *Pax1*, but also additional gene(s) within or nearby the deletion interval. Remarkably, despite the potential involvement of additional gene(s) other than *Pax1*, only the derivatives of embryonic *Pax1*-positive tissues are affected in *Pax1*^{Uns} mutant mice. This characteristic feature of *Pax1*^{Uns} allowed us to propose two different, but not mutually exclusive, hypotheses (WILM *et al.* 1998): First, a gene or genes sharing expression domains with *Pax1* are ablated by the *Pax1*^{Uns} deletion ("co-deletion model"). Second, a gene or genes flanking the *Pax1*^{Uns} deletion interval come under the influence of regulatory elements of *Pax1*, thereby being ectopically activated in the natural expression domains of *Pax1* ("ectopic activation model").

In the present study, we delineated the molecular basis of the *Pax1*^{Uns} mutation by determining the *Pax1*^{Uns} deletion interval and by analyzing genes around *Pax1*. Our results led us to a conclusion that the *Pax1*^{Uns} deletion mutation affects physically linked *Pax1*, *Nkx2-2*, and their potential antisense genes, leading to a contiguous gene syndrome due to a loss-of-function mutation of *Pax1* and a gain-of-function mutation of *Nkx2-2*.

MATERIALS AND METHODS

Animals: *Pax1*^{Uns} mutant mice were kindly provided by A. M. Malashenko (Krosnogorsk, Russia). *Pax1*^{null} mutant mice (referred to as *Pax1*^{tm1neu} with Mouse Genome Informatics (MGI) accession ID MGI:185756 in Mouse Genome Database) were generated and genotyped as described (WILM *et al.* 1998). These mutant strains have been maintained as congenic lines on the C57BL/6J background.

Bacterial artificial chromosome (BAC) library screening: The CitbCj7 mouse BAC library of 129/Sv origin was purchased from Research Genetics (Huntsville, AL). A total of 10 BAC clones were isolated in multiple rounds of screening by hybridization with a 1-kb *Xba*I fragment from intron 2 of *Pax1* (Figure 1) and subsequently with a mixture of two BAC-end fragments (see below) originating from BAC213 (the T7 end, 5' of *Pax1*) and BAC132 (the T7 end, 3' of *Pax1*). In addition, 8 *Pax1*-positive BAC clones including RP23-224L16 and RP23-382B13 were isolated from the RPCI-23 C57BL/6J library (Research Genetics).

BAC-end cloning: pBeloBAC11-based clones from the CitbCj7 BAC library were digested with *Not*I and *Bgl*II, and the resulting fragments in mixture were subcloned into *Not*I-*Bam*HI cleaved pBluescriptII KS (Stratagene, La Jolla, CA). BAC-end subclones were identified by Southern hybridization with two *Not*I-*Hind*III vector fragments, each of which contained either the T7 or the SP6 priming site and flanked the *Hind*III cloning site of pBeloBAC11. Identified BAC-end subclones were sequenced to design PCR primers for sequence-tagged sites (STSs). The primers for the STSs (designated as D2Neu#) are as listed (see online supplemental Table 1 available at <http://www.genetics.org/supplemental/>).

BAC transgenesis: pBeloBAC11-based BAC clones were linearized at the cosN site by λ -terminase (Takara, Berkeley, CA). Linear BAC DNA was separated by pulsed-field gel electrophoresis (PFGE), electroeluted from 1% agarose PFGE gel, and used for the production of transgenic mice. Transgenic mice were generated by pronucleus injection of linearized transgene constructs into fertilized eggs that were subsequently

transferred into the oviducts of pseudopregnant fosters. The presence of both ends of the BAC transgenes was confirmed by PCR with two primer sets specific for the T7 end (5'-CAATG GAAGTCCGAGCTC-3' and 5'-GTGACTCTAGAGGATC-3') and for the SP6 end (5'-CCGCTCACAAATCCACACA-3' and 5'-CCGGCAGTTTCTACACAT-3').

Determination of the *Pax1*^{Uns} deletion interval: To clone a segment flanking the deletion interval from *Pax1*^{Uns} genomic DNA, a cassette-ligation-mediated PCR method, originally described as a cDNA cloning method by ISEGAWA *et al.* (1992), was adapted as follows. All primer sequences used for this procedure are as listed (see online supplemental Table 2 available at <http://www.genetics.org/supplemental/>). Two nested forward primers, Un-s1 and Un-s2, were derived from a region downstream of the 3' deletion breakpoint (see RESULTS). *Eco*RI-digested total genomic DNA (500 ng) from *Pax1*^{Uns} homozygous animals was ligated to preannealed *Eco*RI linkers, linker 1 and linker 2 (4 pmol each), which harbored sequences for nested reverse PCR primers, rev1 and rev2. One-tenth of each reaction was incubated for 10 min at 94° and subsequently subjected to the first PCR amplification with 1.1 mM Mg(OAc)₂, 1 M GC-Melt, 1× reaction buffer, 1/50 *Tth* polymerase mix (Advantage-GC genomic PCR kit from CLONTECH, Palo Alto, CA), and 10 μM primer mix (Un-s1/rev1) under the following conditions: 4 min 94° (initial denaturing); 35 cycles of 30 sec at 94°, 5 min at 68° (two-step amplification); and 5 min at 68° (final extension). One-fiftieth of the first PCR reaction was diluted 1:10 and subjected to the second PCR amplification using the same conditions with primer combinations (Un-s2/rev2). The resulting PCR fragments were cloned with the TOPO TA cloning kit (Invitrogen, San Diego).

Computational analysis of genome sequences: Web-based tools at the National Center for Biotechnology Information (NCBI; <http://www.ncbi.nlm.nih.gov>), including BLAST programs and the GenBank databases, were used for gene search on genomic sequences. Repetitive sequences were masked by using RepeatMasker (<http://ftp.genome.washington.edu/RM/RepeatMasker.html>). Genome annotation data were surveyed at the Ensemble Genome Server (<http://www.ensembl.org>) and the NCBI.

Whole-mount *in situ* hybridization: For genotyping embryos for this analysis, multiplex PCR amplification was performed with two forward primers (Un-s FW: 5'-AGACATGCCACAGTA TTCCC-3' and Un-s FM: 5'-ACATCCATCCAGAGACATGC-3') and one common reverse primer (Un-s RC: 5'-ATGTCCTAGAG ATCCACAGC-3') in single reactions. This PCR amplification produces two diagnostic products specific for either the *Pax1*^{Uns} (463 bp) or the wild-type (611 bp) allele (see Figure 3D). Mouse *Pax1* (NEUBÜSER *et al.* 1995), *Nkx2-2* (PABST *et al.* 1998), and *Bapx1* (LETTICE *et al.* 2001) RNA probes were labeled with digoxigenin and developed with BM purple (Roche). A probe specific for *Pax1* exon 0 was generated from the 465-bp PCR fragment using the following primers: 5'-AACATTAGG GTCCCTCCATTCACG-3' and 5'-GCAAAGTGTCTCTTCAACT TTCCG-3'. Whole-mount *in situ* hybridization was performed according to the protocol of SPÖRLE and SCHUGHART (1998). Control embryos were hybridized with a sense probe to verify the specificity of the antisense probe signal.

RESULTS

Transcription start sites of *Pax1* and identification of a novel 5' exon: Alignment of a 17,615-bp genome sequence, including mouse *Pax1* from this study (GenBank accession no. AF285175), with the published cDNA sequence (GenBank accession no. NM_008780) deter-

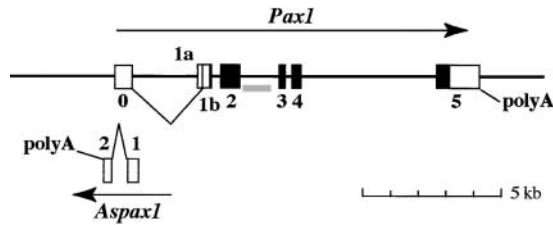


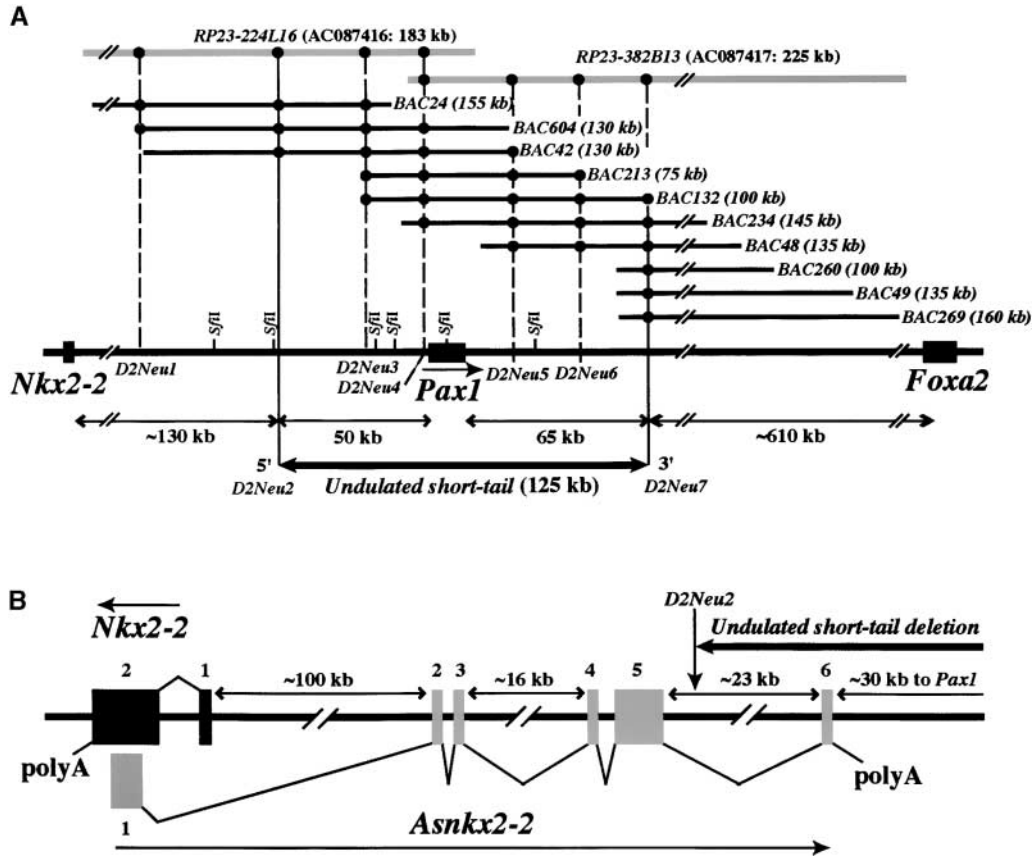
FIGURE 1.—Genomic organization of mouse *Pax1* and its potential antisense gene *Aspax1*. Exons are numbered (0–5 for *Pax1* and 1–2 for *Aspax1*) and indicated by boxes (open box, UTR; solid box, coding region). The last exons are indicated by the presence of poly(A) signals. Note the alternative usage of exon 1: 1a and 1b (see RESULTS). Transcriptional orientations of *Pax1* and *Aspax1* are shown by the arrows. The sequenced region (AF285175) is indicated by the solid line. The 1.0-kb *XbaI* fragment in intron 2 used for BAC library screening is depicted by the shaded bar.

mined the general genomic organization of five exons of mouse *Pax1*, spanning a 10-kb genome region (Figure 1). Putative transcription start sites of *Pax1* were defined by sequencing five *Pax1* cDNA clones that were retrieved from the RIKEN full-length enriched cDNA libraries (CARNINCI *et al.* 2000). In four of them, the 5' untranslated regions (UTRs) extended 66 bases upstream from the published 5' end (NM_008780), leading to the determination of the 5' end of exon 1 (exon 1a in Figure 1; GenBank accession no. AB080656). The remaining clone (RIKEN clone ID 5832428N23; GenBank accession no. AB080657) contained a 5' UTR that was 630 bp longer than the published sequence and included a novel exon (referred to hereafter as exon 0). Exon 0 is located ~2.5 kb upstream of exon 1 and splices into the inside of exon 1 (exon 1b in Figure 1). Thus this type of *Pax1* transcript lacks the 5' part of the exon 1. The splicing between exons 0 and 1b completely follows the GT-AG rule (MOUNT 1982). Furthermore, expression of this version of *Pax1* transcripts was confirmed by whole-mount *in situ* hybridization with a probe specific for exon 0, showing a pattern identical to that with a conventional *Pax1* probe (data not shown). Thus we conclude that there are two alternative forms of *Pax1* transcripts with either of the two transcription start sites: one at the 5' end of exon 0 or the other at the 5' end of exon 1a. Resulting *Pax1* transcripts differ in the structure of the 5' UTR, but the coding sequences are identical.

BAC contig map encompassing the *Pax1* locus: We established a BAC contig map of ~400 kb encompassing mouse *Pax1* (Figure 2A). Ten clones including five *Pax1*-positive BACs and their overlapping clones were isolated from the CitbCj7 mouse BAC library. Restriction mapping with *SfiI* digestion and BAC-end STS mapping (see online supplemental Table 1 available at <http://www.genetics.org/supplemental/>) allowed us to determine the relative order and orientation of the BAC clones.

Furthermore, we isolated two additional BAC clones (RP23-224L16 and RP23-382B13) with larger inserts from the RPCI-23 library and added them to this contig map for the subsequent sequence analysis (see below).

Determination of the *Pax1*^{Uns} deletion interval: In the following descriptions, we refer to the 5' end and the 3' end of a deletion interval as “5' breakpoint” and “3' breakpoint,” respectively. We tested several BAC-end fragments as probes for Southern hybridization on *Pax1*^{Uns} and wild-type genomic DNA to determine the extent of the *Pax1*^{Uns} deletion. Remarkably, an 800-bp *PstI* fragment from the T7-end clone of BAC132 (10 kb), located ~60 kb downstream of *Pax1* (Figure 2), gave no signal on homozygous *Pax1*^{Uns} genomic DNA (Figure 3A). This indicates that this region is included in the *Pax1*^{Uns} deletion interval. On the other hand, an STS marker, *D2Neu7*, which is also derived from the same BAC132 T7-end clone and located ~5 kb downstream of the *PstI* fragment, is present in the *Pax1*^{Uns} genome (data not shown). We subcloned a 2.4-kb *EcoRI* fragment positive for *D2Neu7* from the BAC132 T7-end clone. Genomic Southern analysis with this 2.4-kb *EcoRI* probe demonstrated a rearrangement in the *Pax1*^{Uns} genome (Figure 3B), indicating that the 2.4-kb *EcoRI* fragment included the 3' breakpoint of *Pax1*^{Uns}. We determined the sequence of the 2.4-kb fragment and designed the primers Un-s1 and Un-s2 for the cassette-ligation-mediated PCR method (see MATERIALS AND METHODS and online supplemental Table 2 available at <http://www.genetics.org/supplemental/>). This method allowed us to isolate a 2.2-kb genomic fragment including segments that flanked the deletion interval from homozygous *Pax1*^{Uns} genomic DNA. The sequence comparison of the *Pax1*^{Uns}-derived 2.2-kb fragment with the wild-type-derived 2.4-kb *EcoRI* fragment determined the 3' breakpoint (Figure 3E). For the identification of the 5' breakpoint, we then established the STS marker *D2Neu2* (Figure 2A and online supplemental Table 1 available at <http://www.genetics.org/supplemental/>) from a part of the 2.2-kb fragment flanking the deletion interval on the 5' side. We subcloned a *D2Neu2*-positive 2-kb *HindIII* fragment from BAC42. Genomic Southern analysis with the 2-kb *HindIII* fragment as a probe detected a rearrangement in the *Pax1*^{Uns} genomic DNA (Figure 3C), indicating that the 2-kb *HindIII* fragment included the 5' breakpoint. Sequence comparison of the *Pax1*^{Uns}-derived 2.2-kb fragment with the wild-type-derived 2-kb *HindIII* fragment determined the 5' breakpoint (Figure 3E). No further alterations such as insertions or inversions were confirmed in the *Pax1*^{Uns} mutation by sequence comparison and by Southern analysis. Analysis of mouse *Pax1*-positive BAC sequences (see below) located the 5' breakpoint 50 kb upstream of exon 1 and the 3' breakpoint 65 kb downstream of exon 5. Consequently, the entire length of the *Pax1*^{Uns} deletion interval is ~125 kb (Figure 2A). To facilitate the genotyping of the *Pax1*^{Uns} mutants, we established a



indicated by boxes: solid ones for *Nkx2-2* and shaded ones for *Asnmx2-2*. The last exons are indicated by the presence of poly(A) signals. Transcriptional orientations are indicated by the arrows above the gene names. The *Asnmx2-2* exons distribute in a 148-kb genome interval. Approximate sizes of large intervals (indicated by gaps) are given in kilobases. Note that the first exon of *Asnmx2-2* overlaps with the second exon of *Nkx2-2* in an antisense orientation and that the last exon of *Asnmx2-2*, located ~30 kb upstream of exon 0 of *Pax1*, is included in the 5' part of the *Pax1*^{Ums} deletion interval (bold horizontal bar with an arrow). The STS marker *D2Neu2* defines the 5' breakpoint of the *Pax1*^{Ums} deletion interval.

PCR-based genotyping assay using three specific primers (Figure 3D).

Genes around *Pax1*: Two overlapping mouse BAC clones, RP23-224L16 (183 kb) and RP23-382B13 (225 kb), encompassing the *Pax1* locus were sequenced through the National Institutes of Health (NIH)-funded Genome Sequencing Network (Trans-NIH Mouse Initiative) upon our proposal (Figure 2A; GenBank accession nos. AC087416 and AC087417). By BLAST search we looked for genes and potential genes represented by expressed sequence tags (ESTs) in a 350-kb genomic region covered by the two BAC sequences. Aside from *Pax1* itself, we hit one EST cluster showing significant homology to a segment of the genome sequence, which is located 2.3 kb upstream of *Pax1* exon 1. This EST cluster consists of seven ESTs (representatively, GenBank accession nos. AI646519, BF019981, and AI608217) derived from three independent cDNA clones (IMAGE: 1226169, 3470654, and 789910). By sequencing the entire insert of these overlapping clones, we obtained a 752-bp consensus sequence (GenBank accession no.

AB080658), which consists of two exons perfectly corresponding to nucleotides 1698–1985 and 2504–2946 of the mouse *Pax1* genome sequence AF285175 (Figure 1). The presence of a poly(A) stretch and the consensus splicing signals GT/AG indicates that the 752-bp fragment is part of a real gene. Notably, this gene overlaps with *Pax1* exon 0 by 183 nucleotides in an antisense orientation (Figure 1). This gene does not appear to have a real open reading frame, because the sequence contains a number of stop codons in all three reading frames. These data suggest that this gene is a noncoding antisense gene for *Pax1* (thus referred to hereafter as *Aspax1*). The complete primary structure and function of *Aspax1* remains to be elucidated.

Extending our gene search, we examined the mouse genome sequence maps (NCBI: <http://www.ncbi.nlm.nih.gov> and EBI: <http://www.ensembl.org>). We found *Nkx2-2* and *Foxa2* (formerly *Hnf3β*) located ~180 kb upstream and 672 kb downstream of *Pax1*, respectively (Figure 2A). According to the annotation for the mouse chromosome 2 genome sequence (NW_000178), there are four (LOC

FIGURE 2.—(A) BAC contig map encompassing mouse *Pax1*. The bold horizontal bars represent 10 BAC clones from the CitbCJ7 mouse BAC library. The shaded horizontal bars represent two sequenced BAC clones from the RPCI-23 mouse BAC library. The solid boxes indicate the regions including exons of *Pax1*, *Nkx2-2*, or *Foxa2*. The orientation of the contig is according to the transcriptional orientation of *Pax1*. Seven STS markers from this study, *D2Neu1*–*D2Neu7*, are shown according to their locations and presence on BAC clones (marked by the solid circles). The deletion interval in *Pax1*^{Ums} (between *D2Neu2* and *D2Neu7*) is indicated by the bold arrow. *Sfi* sites within the interval between *D2Neu1* and *D2Neu7* are included. (B) Genomic organization of mouse *Nkx2-2* and its potential antisense gene *Asnmx2-2*. Exons are numbered (1–2 for *Nkx2-2* and 1–6 for *Asnmx2-2*) and

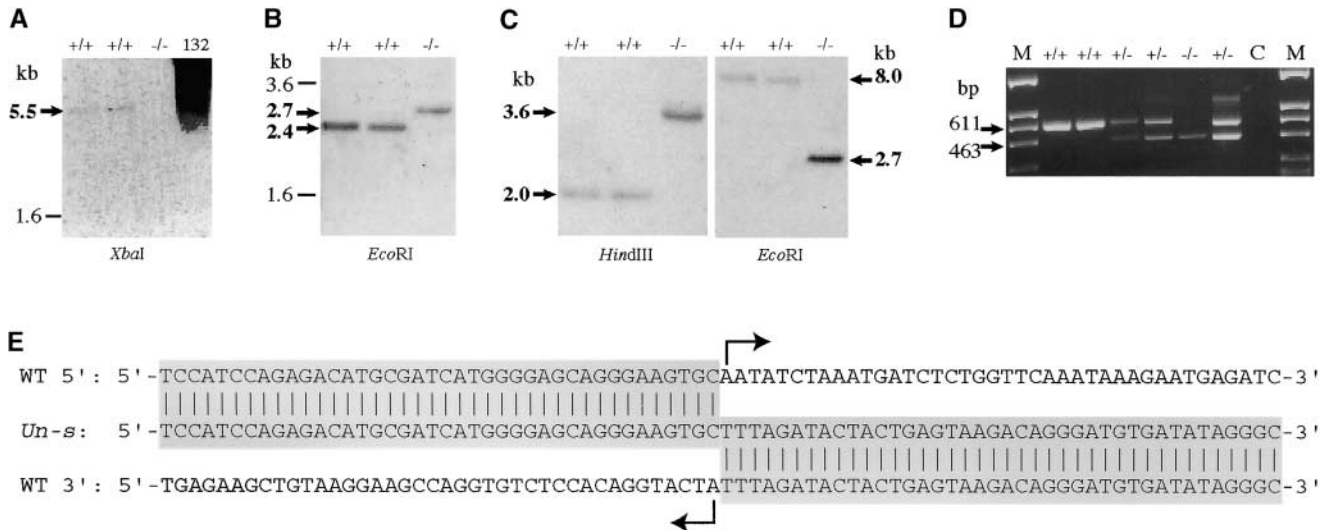


FIGURE 3.—Analysis and determination of the *Pax1*^{Uns} deletion interval. (A) Southern blot analysis of the *Pax1*^{Uns} genome with an 800-bp *PstI* fragment from the 3' end clone of BAC132 as a probe. Note that the 5.5-kb signal is absent in *Pax1*^{Uns} homozygote DNA (-/-). (B) Southern blot analysis of the *Pax1*^{Uns} genome with a 2.4-kb *D2Neu7*-positive *EcoRI* fragment as a probe, which is ~5 kb downstream of the 800-bp *PstI* segment used as a probe in A. A positive signal in *Pax1*^{Uns} homozygote DNA is detected at 2.7 kb, which is larger than that in wild-type DNA (2.4 kb). (C) Southern blot analysis of the *Pax1*^{Uns} genome with a 2.0-kb *D2Neu2*-positive *HindIII* fragment as a probe. Positive signals in *Pax1*^{Uns} homozygote DNA are detected at 3.6 kb (*HindIII* digest) and 2.7 kb (*EcoRI* digest), which are different in size from those detected in wild-type DNA (2.0 kb and 8.0 kb, respectively). (D) PCR detection of the *Pax1*^{Uns} allele. M, size marker; C, negative control with water as template. (E) Deletion breakpoints in the *Pax1*^{Uns} mutation. Forty nucleotides upstream and downstream of the deletion breakpoints are shown in comparison with wild-type sequences. Matched nucleotides are indicated by the vertical bars, and regions flanking the deletion interval are marked by shading. The first and the last nucleotides of the deletion intervals are marked by the angled arrows.

241703, LOC241704, LOC228736, and LOC228737) and six (LOC241705, LOC228740, LOC228742, LOC241706, LOC241707, and LOC241708) potential genes in the intervals between *Nkx2-2* and *Pax1* and between *Pax1* and *Foxa2*, respectively. *Aspax1* is not annotated in NW_000178. These putative genes are proposed as gene models on the basis of computer predictions. However, with the exception of LOC228737, no experimental data or EST evidence support the predictions. By further BLAST analysis, the LOC228737 sequence (XM_149219: 650 bases) turned out to correspond to the 3' part of a full-length RIKEN cDNA sequence (AK045921: 4346 bases). By comparing AK045921 with the genome sequence (NW_000178), we found that the AK045921 gene consisted of six exons, spanning over an ~150-kb genome interval between *Nkx2-2* and *Pax1* (Figure 2B). Interestingly, the 5' part of AK045921 (nucleotides 2–281) overlaps to part of *Nkx2-2* (nucleotides 798–1077 of NM_010919) in an antisense orientation (Figure 2B). AK045921 does not appear to contain an open reading frame, as there are a number of stop codons in all three reading frames. Thus, AK045921 may represent a noncoding antisense gene for *Nkx2-2* (thus referred to hereafter as *Asnkx2-2*).

In summary, we found *Nkx2-2* and *Foxa2* as the nearest known genes on either side of *Pax1*. In the interval between *Nkx2-2* and *Pax1*, we confirmed the presence of two genes, *Asnkx2-2* and *Aspax1*, and they may be

noncoding antisense genes for *Nkx2-2* and *Pax1*, respectively. The *Pax1*^{Uns} deletion ablates the last exon of *Asnkx2-2*, at least two known exons of *Aspax1*, and all exons of *Pax1* (Figure 2B).

BAC transgenic rescue: We performed the BAC transgenic rescue experiment with three *Pax1*-positive clones, BAC42 (130 kb), BAC213 (75 kb), and BAC132 (100 kb), which together covered the *Pax1*^{Uns} deletion interval (Figure 2A). We established several BAC transgenic lines (BAC42, four lines; BAC213, one line; BAC132, two lines) and crossed transgenic mice with *Pax1*^{Uns} mice. We could not observe any rescue of the *Pax1*^{Uns} phenotype in the presence of a BAC transgene in heterozygous *Pax1*^{Uns} mice.

Ectopic expression of *Nkx2-2* in *Pax1*^{Uns} mutants: We examined expression of *Nkx2-2* in *Pax1*^{Uns} mutant embryos at E10.5 by whole-mount *in situ* hybridization (Figure 4). *Nkx2-2* is normally expressed in the ventral region of the neural tube adjacent to the floor plate (PRICE *et al.* 1992; Figure 4, A and F). Notably, *Nkx2-2* is ectopically upregulated in the sclerotome compartment of somites and in limb buds of *Pax1*^{Uns} mutant embryos (Figure 4, C, D, H, and I). Normally, *Pax1* is expressed in both of these embryonic tissues (Figure 4, E and J). Expression of *Nkx2-2* in the neural tube is not affected in *Pax1*^{Uns} mutants. Interestingly, ectopic expression of *Nkx2-2* is not detected in the pharyngeal pouch endoderm, another expression domain of *Pax1*.

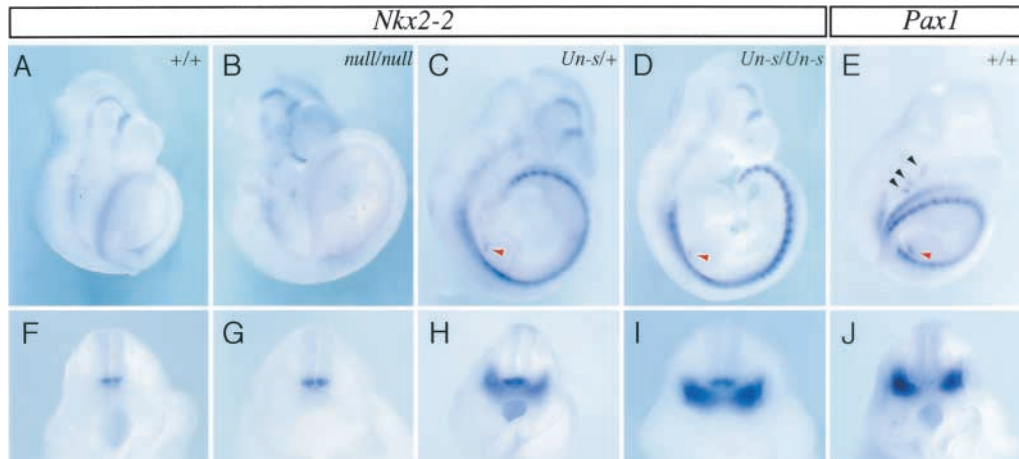


FIGURE 4.—Ectopic expression of *Nkx2-2* in somites and limb buds of *Pax1*^{Un-s} mutants. Whole-mount *in situ* hybridization shows expression of *Nkx2-2* (A–D and F–I) and *Pax1* (E and J) in wild-type (A, E, F, and J), *Pax1*^{null/null} (B and G), *Pax1*^{Un-s/+} (C and H), and *Pax1*^{Un-s/Un-s} (D and I) embryos at E10.5. (F–J) Transverse views at the level of the upper thoracic region. The red arrowheads in C and D indicate ectopic expression of *Nkx2-2* in forelimb buds. The red and black arrowheads in E point to normal *Pax1* expression in the forelimb buds and pharyngeal pouch endoderm, respectively.

Since *Pax1*^{null} homozygous embryos do not exhibit such ectopic expression of *Nkx2-2* (Figure 4, B and G), *Pax1* deficiency itself cannot account for this phenomenon. Comparison of *Pax1*^{Un-s} heterozygotes (Figure 4, C and H) with homozygotes (Figure 4, D and I) demonstrated that the level of *Nkx2-2* expression in these ectopic sites increases depending on the copy number of the mutant allele, suggesting that a *cis*-acting mechanism drives this ectopic activation of *Nkx2-2*. We also examined expression of *Foxa2* in *Pax1*^{Un-s} mutant embryos at E10.5, but we could not detect any change in its expression (data not shown).

Downregulation of *Bapx1* in the sclerotome of *Pax1*^{Un-s} mutants: Another homeobox transcription factor of the NK-2 type, *Bapx1* (or *Nkx3-2*), has been shown to be a major mediator of Shh signaling to induce sclerotome chondrogenesis (MURTAUGH *et al.* 2001). Furthermore, it has been recently identified as a transcriptional target of *Pax1* and its paralog *Pax9* (RODRIGO *et al.* 2003). The results from these studies together suggest that the main role of *Pax1* (and *Pax9*) in sclerotome development is to activate its downstream effector *Bapx1*. Thus we examined

expression of *Bapx1* in *Pax1*^{Un-s} mutant embryos (Figure 5). In targeted *Pax1*^{null} mutants, *Bapx1* expression is either unchanged in heterozygotes or only slightly reduced in homozygotes as a result of compensation by *Pax9* (RODRIGO *et al.* 2003). In contrast, in *Pax1*^{Un-s} mutants, expression of *Bapx1* is significantly reduced, which is already apparent in *Pax1*^{Un-s} heterozygous mutants (Figure 5B) and is even more prominent in *Pax1*^{Un-s} homozygous mutants (Figure 5C).

DISCUSSION

To explain the characteristic features of the *Pax1*^{Un-s} deletion mutation, we previously proposed two working hypotheses: the co-deletion model and the ectopic activation model (WILM *et al.* 1998). In the present study, we determined the deletion interval and clarified the molecular lesion of the *Pax1*^{Un-s} mutation. Our results indicate that the *Pax1*^{Un-s} mutation affects four genes within or nearby the deletion: *Pax1*, *Nkx2-2*, *Asnkx2-2*, and *Aspax1*. We have shown that the *Pax1*^{Un-s} deletion ablates all exons of *Pax1*, the last exon of *Asnkx2-2*, and

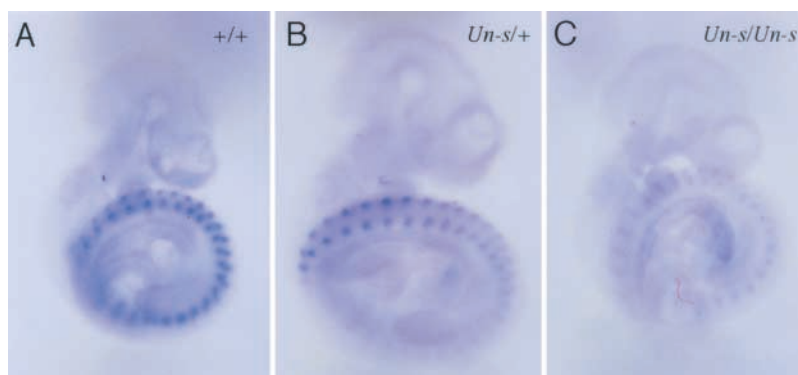


FIGURE 5.—Downregulation of *Bapx1* in the sclerotome of *Pax1*^{Un-s} mutants. Whole-mount *in situ* hybridization shows expression of *Bapx1* in (A) the control (+/+), (B) heterozygotes (*Un-s/+*), and (C) homozygotes (*Un-s/Un-s*) at E10.5. Note that the positive staining in homozygotes is significantly reduced (C). A slight reduction in *Bapx1* expression is recognized in heterozygotes, especially in the anterior part of the trunk (the cervical-to-thoracic regions; B).

at least the last two exons of *Aspax1*. Furthermore, we have demonstrated that in *Pax1^{Un-s}* mutants *Nkx2-2* is ectopically activated in normally *Pax1*-positive domains. Thus, the *Pax1^{Un-s}* mutation leads to both the co-deletion and the ectopic activation of additional genes. Nevertheless, the co-deletion of *Asnknx2-2* and *Aspax1* may not contribute significantly to the *Pax1^{Un-s}* phenotype. *Asnknx2-2* and *Aspax1* are most probably noncoding antisense genes for *Nkx2-2* and *Pax1*, respectively. Noncoding antisense RNA genes are usually involved in post-transcriptional regulation (EDDY 2001; ERDMANN *et al.* 2001). If this were the case, *Asnknx2-2* and *Aspax1* would function only in the context of the functions of their respective sense genes. Indeed, *Asnknx2-2* is unlikely to have other functions that are not related to *Nkx2-2*. The knockout allele of *Nkx2-2* reported by SUSSEL *et al.* (1998) was created by deleting both exon 1 and exon 2 of *Nkx2-2*, the latter of which contained exon 1 of *Asnknx2-2* (see Figure 2B). Thus, this strategy inactivates both *Nkx2-2* and *Asnknx2-2* at the same time. Nevertheless, the observed defects in the knockout mutants are all related to *Nkx2-2*-positive tissues, strongly suggesting that *Asnknx2-2* functions in the context of *Nkx2-2* or that *Asnknx2-2* is dispensable. The disturbance of *Asnknx2-2* alone could lead to an enhanced translation of *Nkx2-2*, but this effect is possible only when *Nkx2-2* sense mRNA is present. Therefore, the ectopic expression of *Nkx2-2* should play a primary role, and the contribution by the disturbance of *Asnknx2-2*, if at all, should be secondary. Likewise, the disruption of *Aspax1* and *Pax1* at the same time may not result in a mutant allele with a more extreme phenotypic effect than that of a *Pax1* deficiency. In any event, the functions of *Asnknx2-2* and *Aspax1* have to be determined in future studies to assess the contributions of these two genes to the *Pax1^{Un-s}* phenotype. Currently, we are not able to determine their expression profiles by Northern and *in situ* hybridization analyses, suggesting that they are expressed at low levels and/or that their transcripts are unstable, which is often the case with antisense RNA genes (STORZ 2002). In addition, our result from the BAC transgenic rescue experiment does not support the presence of more genes within the deletion interval that contribute to the *Pax1^{Un-s}* phenotype.

On the other hand, ectopic expression of *Nkx2-2* in the somites and limb buds of *Pax1^{Un-s}* mutant embryos is remarkable and strikingly similar to normal expression of *Pax1*. Thus, this result suggests that *cis*-regulatory elements or enhancers, which normally direct *Pax1* expression, still remain in the *Pax1^{Un-s}* genome and drive expression of *Nkx2-2* in *Pax1^{Un-s}* mutants. *Pax1* and *Nkx2-2* show different and discrete expression profiles in the wild-type situation. Therefore, we can assume an insulation mechanism that limits enhancer activities of *Pax1* or *Nkx2-2* enhancers to their respective genes. We propose a model to explain how the *Pax1*-like expression of *Nkx2-2* in *Pax1^{Un-s}* mutants occurs, as depicted in Figure 6 (insulator model). In this model, the enhancers that direct expression of *Pax1*

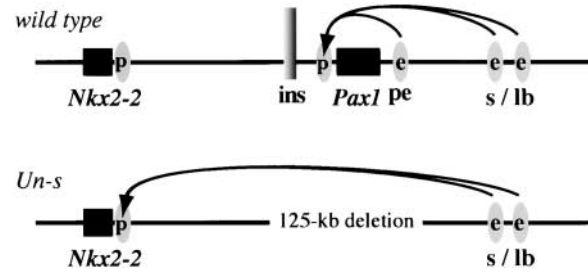


FIGURE 6.—A model for the mechanism of ectopic activation of *Nkx2-2* in *Pax1^{Un-s}* mutants. Enhancers (e) of *Pax1* expression in the pharyngeal pouch endoderm (pe), somites (s), and limb buds (lb) are indicated by ovals. Note that in this model pe is located inside the *Pax1^{Un-s}* deletion, while the s and lb enhancers reside distal to the 3'-deletion breakpoint. In the wild-type situation, a putative *cis*-element or insulator (ins) directs the interaction of the *Pax1* enhancers only with the promoter (p) of *Pax1*, not with the *Nkx2-2* promoter, thereby establishing a boundary between *Pax1* and *Nkx2-2*. The *Pax1^{Un-s}* deletion eliminates all exons and the promoter of *Pax1*, together with the pe enhancer and the insulator, thus allowing the s and lb enhancers to interact with the *Nkx2-2* promoter.

in the somites and limb buds are located outside the deletion interval, *i.e.*, >65 kb downstream of *Pax1* in the wild-type genome. Consistent with this assumption, we could not see any rescue for the skeletal defects in *Pax1^{null}* mutants by the BAC transgenes (BAC42, BAC 213, and BAC132; see Figure 2A) in multiple lines, suggesting that the BAC intervals defined by the *Pax1*-positive BAC clones do not contain *cis*-regulatory elements sufficient for the expression of *Pax1* in the sclerotome and the limb buds. Furthermore, in this model we assume that some *cis*-element that defines a boundary between *Pax1* and *Nkx2-2* is located up to 50 kb upstream of *Pax1*. Such a *cis*-element can be regarded as an insulator, as defined in a recent review (WEST *et al.* 2002). This insulator blocks the action of the *Pax1* enhancers on the *Nkx2-2* promoter in the normal situation (Figure 6, top). In *Pax1^{Un-s}* mutants, the insulator is ablated by the deletion, thereby allowing the *Pax1* enhancers to illegitimately communicate with the *Nkx2-2* promoter (Figure 6, bottom). On the other hand, the absence of ectopic *Nkx2-2* in the pharyngeal pouch endoderm of *Pax1^{Un-s}* embryos suggests that the *Pax1* pharyngeal pouch endoderm enhancer is located within the *Pax1^{Un-s}* deletion interval. Alternative to this insulator model, the insulation mechanism might be established simply by the distance between the two loci. If it is the case, the shortened distance between the *Nkx2-2* promoter and the *Pax1* enhancers would account for the regulatory interference in the *Pax1^{Un-s}* allele, although this explanation is inconsistent with a distance-independent manner of enhancer actions (BLACKWOOD and KADONAGA 1998). The molecular basis of the gene insulation here remains to be elucidated in future studies.

What could ectopically expressed *Nkx2-2* lead to?

Since *Nkx2-2* is implicated in the cell-type specification during the development of the central nervous system and pancreatic islets (SUSSEL *et al.* 1998; BRISCOE *et al.* 1999; McMAHON 2000; QI *et al.* 2001; SOULA *et al.* 2001), ectopic expression of *Nkx2-2* might have a potential to change the fate of sclerotomal cells. We tested this possibility by examining expression of *Nkx6-1* as a marker that is often coexpressed by *Nkx2-2*-positive cells in the ventral neural tube (McMAHON 2000) and in the pancreas (SANDER *et al.* 2000), but we could not detect any change in *Nkx6-1* expression (data not shown). Thus it seems unlikely that cells with ectopic expression of *Nkx2-2* in *Pax1^{Un-s}* mutants change their fates.

We have demonstrated that *Bapx1* (or *Nkx3-2*) is downregulated more significantly in *Pax1^{Un-s}* mutants than in *Pax1*-null mutants. Since *Bapx1* is the main effector of Shh signaling to induce sclerotome chondrogenesis (MURTAUGH *et al.* 2001), this observation accounts well for the difference in the phenotype severity between the *Pax1^{Un-s}* and *Pax1*-null mutations. *Bapx1* is a downstream target of Pax1 and Pax9, but *Bapx1* expression in *Pax1*-null mutants is only slightly reduced due to the compensation by Pax9 (RODRIGO *et al.* 2003). Therefore, in addition to the loss of *Pax1*, there must be an additional mechanism that results in the enhanced downregulation of *Bapx1* in *Pax1^{Un-s}*. We assume that ectopically activated *Nkx2-2* may fulfill this role. *Bapx1* and *Nkx2-2* are NK homeobox transcription factors and share a high degree of structural similarities, including the presence of the TN domain, NK2 homeodomain (characterized by the presence of tyrosine at homeodomain position 54), and NK2-specific domain (NK2-SD; TRIBIOLI *et al.* 1997). It has been shown that *Bapx1* acts as a transcriptional repressor to exert its chondrogenic function in the sclerotome (MURTAUGH *et al.* 2001). *Bapx1* can be converted into a transcriptional activator by appending a strong activator domain from VP16 (designated as *Nkx3.2-VP16* in MURTAUGH *et al.* 2001). When *Nkx3.2-VP16* is overexpressed in chick somites, sclerotome chondrogenesis is inhibited (MURTAUGH *et al.* 2001) and expression of endogenous *Bapx1* is downregulated, due to the disturbance of the positive autoregulatory loop that maintains expression of *Bapx1* (ZENG *et al.* 2002). Thus these defects caused by overexpressed *Nkx3.2-VP16* in somites mirror what we have demonstrated in *Pax1^{Un-s}* mutants, suggesting the possibility that ectopically expressed *Nkx2-2* in the sclerotome may act as a transcriptional activator, thereby interfering with *Bapx1* function. *Nkx2-2* has a potent activator domain at the C-terminal part, and the NK2-SD domain, presumably together with a cofactor, masks the transcriptional activity of this domain (WATADA *et al.* 2000). Therefore, under an abnormal condition (*i.e.*, ectopic expression) the activity of the C-terminal domain may not be properly masked by NK2-SD, leading to transcriptional activation by *Nkx2-2*.

In conclusion, we propose that a combination of the

Pax1 deficiency and the ectopic activation of *Nkx2-2* by the *Pax1* enhancers is the molecular basis of the *Pax1^{Un-s}* mutation. This combined molecular defect accounts for the *Pax1^{Un-s}* phenotype that is significantly enhanced but is restricted to *Pax1*-positive tissues.

We thank M. Karasawa for her technical advice for the deletion interval analysis and H. Hamada and the members of his laboratory for help with whole-mount *in situ* analysis. We acknowledge E. Knapik and J. Favor for critical reading of the manuscript. We also acknowledge R. Hill for the *Bapx1* probe, the Resource Center of the German Human Genome Project for distributing EST clones, and the University of Oklahoma for BAC sequencing through the NIH-funded Genome Sequencing Network. This work was supported in part by grants from the Deutsche Forschungsgemeinschaft and the GSF-National Research Center for Environment and Health, and in part by the Ministry of Education, Culture, Sports, Science and Technology of Japan, with Special Coordinating Funds for Promoting Science and Technology (K.A.).

LITERATURE CITED

- BALLING, R., U. DEUTSCH and P. GRUSS, 1988 *undulated*, a mutation affecting the development of the mouse skeleton, has a point mutation in the paired box of *Pax1*. *Cell* **55**: 531–535.
- BLACKWOOD, E. M., and J. T. KADONAGA, 1998 Going the distance: a current view of enhancer action. *Science* **281**: 60–63.
- BLANDOVA, Z. K., and I. EGOROV, 1975 *Sut* allelic with un. *Mouse News Lett.* **52**: 43.
- BRISCOE, J., L. SUSSEL, P. SERUP, D. HARTIGAN-O'CONNOR, T. M. JESSELL *et al.*, 1999 Homeobox gene *Nkx2.2* and specification of neuronal identity by graded Sonic hedgehog signaling. *Nature* **398**: 622–627.
- CARNINCI, P., Y. SHIBATA, N. HAYATSU, Y. SUGAHARA, K. SHIBATA *et al.*, 2000 Normalization and subtraction of cap-trapper-selected cDNAs to prepare full-length cDNA libraries for rapid discovery of new genes. *Genome Res.* **10**: 1617–1630.
- DAHL, E., H. KOSEKI and R. BALLING, 1997 Pax genes and organogenesis. *Bioessays* **19**: 755–765.
- DEUTSCH, U., G. R. DRESSLER and P. GRUSS, 1988 Pax 1, a member of a paired box homologous murine gene family, is expressed in segmented structures during development. *Cell* **53**: 617–625.
- DIETRICH, S., and P. GRUSS, 1995 *undulated* phenotypes suggest a role of *Pax-1* for the development of vertebral and extraxial structures. *Dev. Biol.* **167**: 529–548.
- EDDY, S. R., 2001 Non-coding RNA genes and the modern RNA world. *Nat. Rev. Genet.* **2**: 919–929.
- ERDMANN, V. A., M. Z. BARCISZEWSKA, M. SZYMANSKI, A. HOCHBERG, N. DE GROOT *et al.*, 2001 The non-coding RNAs as riboregulators. *Nucleic Acids Res.* **29**: 189–193.
- GRÜNEBERG, H., 1950 Genetical studies on the skeleton of the mouse. II. *Undulated* and its “modifiers.” *J. Genet.* **50**: 142–173.
- GRÜNEBERG, H., 1954 Genetical studies on the skeleton of the mouse. XII. The development of *undulated*. *J. Genet.* **52**: 441–455.
- ISEGAWA, Y., J. SHENG, Y. SOKAWA, K. YAMANISHI, O. NAKAGOMI *et al.*, 1992 Selective amplification of cDNA sequence from total RNA by cassette-ligation mediated polymerase chain reaction (PCR): application to sequencing 6.5 kb genome segment of hantavirus strain B-1. *Mol. Cell. Probes* **6**: 467–475.
- LETTICE, L., J. HECKSHER-SORENSEN and R. HILL, 2001 The role of *Bapx1* (*Nkx3.2*) in the development and evolution of the axial skeleton. *J. Anat.* **199**: 181–187.
- MANSOURI, A., G. GOUDREAU and P. GRUSS, 1999 Pax genes and their role in organogenesis. *Cancer Res.* **59**: 1707s–1710s.
- McMAHON, A. P., 2000 Neural patterning: the role of *Nkx* genes in the ventral spinal cord. *Genes Dev.* **14**: 2261–2264.
- MOUNT, S. M., 1982 A catalogue of splice junction sequences. *Nucleic Acids Res.* **10**: 459–472.
- MURTAUGH, L. C., L. ZENG, J. H. CHYUNG and A. B. LASSAR, 2001 The chick transcriptional repressor *Nkx3.2* acts downstream of

- Shh to promote BMP-dependent axial chondrogenesis. *Dev. Cell* **1**: 411–422.
- NEUBÜSER, A., H. KOSEKI and R. BALLING, 1995 Characterization and developmental expression of Pax9, a paired-box-containing gene related to Pax1. *Dev. Biol.* **170**: 701–716.
- PABST, O., H. HERBRAND and H. H. ARNOLD, 1998 Nkx2-9 is a novel homeobox transcription factor which demarcates ventral domains in the developing mouse CNS. *Mech. Dev.* **73**: 85–93.
- PRICE, M., D. LAZZARO, T. POHL, M. G. MATTEI, U. RUTHER *et al.*, 1992 Regional expression of the homeobox gene Nkx-2.2 in the developing mammalian forebrain. *Neuron* **8**: 241–255.
- QI, Y., J. CAI, Y. WU, R. WU, J. LEE *et al.*, 2001 Control of oligodendrocyte differentiation by the Nkx2.2 homeodomain transcription factor. *Development* **128**: 2723–2733.
- RODRIGO, I., R. E. HILL, R. BALLING, A. MUNSTERBERG and K. IMAI, 2003 Pax1 and Pax9 activate *Bapx1* to induce chondrogenic differentiation in the sclerotome. *Development* **130**: 473–482.
- SANDER, M., L. SUSSEL, J. CONNERS, D. SCHEEL, J. KALAMARAS *et al.*, 2000 Homeobox gene Nkx6.1 lies downstream of Nkx2.2 in the major pathway of beta-cell formation in the pancreas. *Development* **127**: 5533–5540.
- SOULA, C., C. DANESIN, P. KAN, M. GROB, C. PONCET *et al.*, 2001 Distinct sites of origin of oligodendrocytes and somatic motoneurons in the chick spinal cord: oligodendrocytes arise from Nkx2.2-expressing progenitors by a Shh-dependent mechanism. *Development* **128**: 1369–1379.
- SPÖRLE, R., and K. SCHUGHART, 1998 Paradox segmentation along inter- and intrasomitic borderlines is followed by dysmorphology of the axial skeleton in the *open brain (opb)* mouse mutant. *Dev. Genet.* **22**: 359–373.
- STORZ, G., 2002 An expanding universe of noncoding RNAs. *Science* **296**: 1260–1263.
- SUSSEL, L., J. KALAMARAS, D. J. HARTIGAN-O'CONNOR, J. J. MENESES, R. A. PEDERSEN *et al.*, 1998 Mice lacking the homeodomain transcription factor Nkx2.2 have diabetes due to arrested differentiation of pancreatic beta cells. *Development* **125**: 2213–2221.
- TIMMONS, P. M., J. WALLIN, P. W. RIGBY and R. BALLING, 1994 Expression and function of Pax 1 during development of the pectoral girdle. *Development* **120**: 2773–2785.
- TRIBIOLI, C., M. FRASCH and T. LUFKIN, 1997 Bapx1: an evolutionary conserved homologue of the Drosophila bagpipe homeobox gene is expressed in splanchnic mesoderm and the embryonic skeleton. *Mech. Dev.* **65**: 145–162.
- WALLACE, M. E., 1980 Undulated alleles. *Mouse News Lett.* **63**: 10.
- WALLIN, J., J. WILTING, H. KOSEKI, R. FRITSCH, B. CHRIST *et al.*, 1994 The role of Pax-1 in axial skeleton development. *Development* **120**: 1109–1121.
- WALLIN, J., H. EIBEL, A. NEUBÜSER, J. WILTING, H. KOSEKI *et al.*, 1996 *Pax1* is expressed during development of the thymus epithelium and is required for normal T-cell maturation. *Development* **122**: 23–30.
- WATADA, H., R. G. MIRMIRA, J. KALAMARAS and M. S. GERMAN, 2000 Intramolecular control of transcriptional activity by the NK2-specific domain in NK-2 homeodomain proteins. *Proc. Natl. Acad. Sci. USA* **97**: 9443–9448.
- WEST, A. G., M. GASZNER and G. FELSENFELD, 2002 Insulators: many functions, many mechanisms. *Genes Dev.* **16**: 271–288.
- WILM, B., E. DAHL, H. PETERS, R. BALLING and K. IMAI, 1998 Targeted disruption of *Pax1* defines its null phenotype and proves haploinsufficiency. *Proc. Natl. Acad. Sci. USA* **95**: 8692–8697.
- WRIGHT, M. E., 1947 Undulated: a new genetic factor in *Mus musculus* affecting the spine and tail. *Heredity* **1**: 137–141.
- ZENG, L., H. KEMPF, L. C. MURTAUGH, M. E. SATO and A. B. LASSAR, 2002 Shh establishes an Nkx3.2/Sox9 autoregulatory loop that is maintained by BMP signals to induce somitic chondrogenesis. *Genes Dev.* **16**: 1990–2005.

Communicating editor: C. KOZAK

